Hydrothermal synthesis of nanocrystalline ZnSe: An *in situ* synchrotron radiation X-ray powder diffraction study

J.-E. Jørgensen [a,*], T.R. Jensen [a], J.C. Hanson [b]

[a] iNANO and Department of Chemistry, University of Aarhus, DK-8000 Århus C, Denmark
[b] Chemistry Department, Brookhaven National Laboratory, Upton, NY 11973, USA

ARTICLE INFO

ABSTRACT

The hydrothermal synthesis of nanocrystalline ZnSe has been studied by *in situ* X-ray powder diffraction using synchrotron radiation. The formation of ZnSe was studied using the following starting mixtures: $Zn+Se+H_2O$ (route A) and $ZnCl_2+Se+H_2O+Na_2SO_3$ (route B). The route A experiment showed that Zn powder starts reacting with water at 134 °C giving ZnO and H_2 followed by the formation of ZnSe which takes place in temperature range from 167 to 195 °C. The route B experiment shows a considerably more complex reaction path with several intermediate phases and in this case the formation of ZnSe starts at 141 °C and ZnSe and Se were the only crystalline phases observed at the end of the experiment where the temperature was 195 °C. The sizes of the nanocrystalline particles were determined to 18 and 9 nm in the route A and B experiments, respectively. Nanocrystalline ZnSe was also synthesized *ex situ* using the route A and B methods and characterized by conventional X-ray powder diffraction and transmission electron microscopy. An average crystalline domain size of ca. 8 nm was determined by X-ray powder diffraction in fair agreement with TEM images, which showed larger aggregates of nanoparticles having approximate diameters of 10 nm. Furthermore, a method for purification of the ZnSe nanoparticles was developed and the prepared particles showed signs of anisotropic size broadening of the diffraction peaks.

1. Introduction

Synthesis of nanometer-sized particles of II–VI semiconducting compounds has attracted a great deal of interest in recent years. This is due to the fact that studies of such particles provide an opportunity to observe, fine tune and modify the relationship between physical properties, size and shape for a given chemical compound [1–4]. The II–VI semiconducting compounds ZnSe and CdSe have large direct band gaps and they are used for e.g. infrared windows. Furthermore, the application of semiconducting nanoparticles for imaging, labelling and sensing in biological research is of utmost importance [5,6]. Several methods have been developed for their synthesis of which the most straightforward is the combination of the pure elements at high temperature. Other synthetic methods include molecular beam epitaxy, metalorganic chemical vapor deposition, organometallic vapor phase epitaxy and mechanochemical synthesis from Zn and Se granules [7–10]. Solvothermal synthetic methods have also been developed for the synthesis of ZnSe and CdSe e.g. using organic solvents such as pyridine. The advantage of the solvothermal methods is that they

are accomplished at relatively low temperatures and pressures. However, organic solvents are usually harmful to the environment and non-toxic solvents would therefore be advantageous for large-scale production. Recently, nanocrystalline ZnSe has been synthesized by different hydrothermal methods and derivatives thereof. Jiao et al. prepared ZnSe quantum dots (QD) hydrothermally using $ZnCl_2$ and Na_2SeO_3 as Zn and Se sources and hydrazine was used as the reducing agent [11]. Oleic acid was added to control the synthesis conditions so that QDs were obtained. Moreover, oleic acid acted as a stabilizing agent to protect the ZnSe QDs by binding to their surface, and as a result it made the QDs easily dispersed in nonpolar solvents because of its nonpolar alkyl groups. Karanikolos et al. prepared ZnSe nanostructures using lyotropic liquid crystals as templates formed by the self-assembly of an amphiphilic block copolymer in the presence of H_2O and a less polar organic solvent [12]. Zinc-acetate and H_2Se gas was used as the Zn and Se source. ZnSe QD, hollow nanospheres, nanotubes and nanolaminates (parallel nanoplates or free-standing quantum wells) were grown at room temperature and the shape and size of the nanocrystals were precisely controlled by altering the structure of the templating phase as well as changing the concentration of the Zn precursor. Furthermore, Mn-doped ZnSe QD have been prepared by solvothermal synthesis using a nucleation-doping strategy by

Pradhan and Peng [13]. These QD were composed of a MnSe core and a ZnSe overcoating layer.

Nanocrystalline ZnSe was synthesized directly form the elements under hydrothermal conditions using water as the reaction medium by Peng et al. [14]. Stoichiometric amounts of Zn or Cd and Se powders were loaded into a Teflon-lined stainless steel autoclave and kept at 180 °C for 24 h without shaking or stirring. Nanocrystallites of ZnSe and CdSe with an average size of 70–100 nm were obtained. In addition, nanocrystalline CdSe has been prepared by direct reaction between Cd ions and a selenosulfate solution and highly luminescent ZnSe(S) alloyed QD have been prepared by a micro-assisted aqueous method [15,16]. We here report the results of an *in situ* synchrotron radiation X-ray powder diffraction study of the synthesis of ZnSe under hydrothermal conditions as well as *ex situ* laboratory experiments. The aim of this study was to elucidate the reaction paths for the formation of these compounds under hydrothermal conditions.

2. Experimental

The *in situ* synchrotron radiation X-ray powder diffraction work was performed at the X7B beam line at NSLS at Brookhaven National Laboratory, USA. The *in situ* experiments were carried out along two routes labelled A and B. A mixture of Zn and Se (molar ratio 1:1) was used in the route A experiment while a mixture of $ZnCl_2$, Se and Na_2SO_3 (molar ratio 1:1:1) was used in the route B experiment. The following chemicals were used in both *in situ* and *ex situ* experiments: Zn, Merck 8789 p.a., $ZnCl_2$, Merck 8816 p.a., Se, Acros 419271000 and Na_2SO_3, Merck 6657. The reactants were mixed with water in a mortar and loaded into quartz capillary tubes with diameters of 0.5 or 0.7 mm and heated by a hot air stream. The temperature of the hot air flow was measured with a chromel–alumel thermocouple placed 2 mm from the capillary. Temperature ranges from 25 to 120 °C and from 25 to 200 °C were used with heating rates of 0.79 and 1.21 °C/min, respectively. Before the experiments, the phase transition and melting point of a sulfur powder sample was measured to calibrate the sample temperature. The results showed good agreement with the desired and measured sample temperature. The capillaries were pressurized with nitrogen (max. 2.5 MPa) to prevent boiling of the solvent. Powder patterns were recorded in the temperature range from room temperature to 200 °C with a counting time of 30–40 s per pattern using an area detector (Model MAR345) and X-ray radiation with a wave length of 0.90371 Å. The wave length was determined from a powder pattern of LaB_6 ($a = 4.1570$ Å). The recorded images were subsequently converted to powder patterns using the FIT2D software package [17]. Identification of the crystalline phases was made by aid of the ICCD database and the card numbers from this database are subsequently given in parenthesis after the formula of the identified phases.

Laboratory experiments (*ex situ*) were also carried out in Teflon-lined stainless steel autoclaves having a volume of 18 mL. The experiments are summarized in Table 1. The autoclaves were in all cases loaded with approximately 1.5 and 2 g of the reaction mixture for the route A and B experiments, respectively, and 12 mL of water or NaOH solution. The autoclaves were then heated for 2 h at 185 °C. The products were washed with water until the washing water was neutral. X-ray powder patterns of the products used for phase identification were recorded on a Stoe Stadi P diffractometer using $CuK\alpha_1$ ($\lambda = 1.54059290(50)$ Å) radiation. Selected samples were also examined on a Bruker D8 X-ray powder diffractometer equipped with an incident Ge monochromator crystal ensuring $CuK\alpha_1$ radiation. Powder patterns were recorded in the 2θ range from 20° to 120° with a step size of 0.02°

Table 1
Hydrothermal synthesis of ZnSe

No.	Reactants (molar ratios)	Temperature (°C)/time (h)	Products
1	$1Zn:1Se:64H_2O$	170/2	Zn, Se, ZnO
2	$1Zn:1Se:64H_2O$	180/24	ZnSe, Se
3	$1ZnCl_2:1Se:1Na_2SO_3:114H_2O$	170/2	Se, $Zn_3O_4S \cdot 3H_2O$
4	$1ZnCl_2:1Se:1Na_2SO_3:114H_2O$	185/2	ZnSe, Se
5	$1ZnCl_2:Se:1Na_2SO_3:114H_2O:2NaOH$	185/2	ZnSe, Se
6	$1ZnCl_2:1Se:1Na_2SO_3:114H_2O$	180/19	ZnSe, Se

Experiments **1** and **2** correspond to route A, whereas experiments **3–6** correspond to route B.

and a counting time of 17 s per point and a single-crystalline silicon disk was used as sample holder. The Stoe WinX^{POW} software package was used for analysis of the recorded X-ray patterns. The average sizes of the crystalline domains of the synthesized ZnSe particles were determined by the use of the Scherrer equation:

$$FWHM = 0.94\lambda/L\cos(\theta)$$

where L is the size of the crystalline domaines and θ is half the Bragg angle 2θ. The determination of the full width at half maximum (FWHM) parameters for these reflections were performed by fitting a pseudo-Voigt function to the measured reflection profiles by the least squares method. The peak position, FWHM and intensity parameters were refined individually for each reflection in the pattern and the obtained FWHM values for these reflections were corrected for the instrumental broadening. The sizes of the crystalline domains were determined by the use of the Scherrer equation. Transmission electron microscopy images (TEM) were recorded on a Philips CM20 electron microscope operated at 200 kV. The sample was suspended in water and a drop of the suspension was deposited on a carbon-coated TEM grid and allowed to dry before investigation.

3. Results and discussion

The formation of ZnSe was studied by two *in situ* diffraction experiments using $Zn+Se+H_2O$ (route A) and $ZnCl_2+Se+H_2O+Na_2SO_3$ (route B) as starting mixtures. The route A experiment corresponds to the method used by Peng et al. [14] while Na_2SO_3 was chosen as the reducing agent in the route B experiment. The use of Na_2SO_3 prevents the evolution of hydrogen originating from the reaction of Zn with water. Initial trial measurements showed that the $Zn+Se+H_2O$ mixture did not react below 100 °C and Fig. 1a shows a stack of powder patterns recorded as the sample was heated from 90 to 200 °C within 60 min and thereafter kept at 200 °C and each pattern was exposed for 30 s. The identification of phases present at different selected temperatures is shows in Fig. 1b. From Figs. 1a and b, it is seen that Zn powder initially reacts with water giving ZnO and H_2 and the formation of ZnO starts at 134 °C, see Eq. (1). The first indication of the formation of ZnSe is observed at approximately 167 °C where the ZnSe (111) reflection at $2\theta = 16°$ appears as seen from Fig. 1a. The Se Bragg peaks disappear at 195 °C as Se is presumably starting to dissolve as a sol at this temperature. The disappearance of solid Se does not seem to influence the rate of formation of ZnSe. It is therefore concluded that the evolved H_2 gas reduces Se both in the solid and sol state. The formed selenide ions react with ZnO to form ZnSe according to the reaction schemes below:

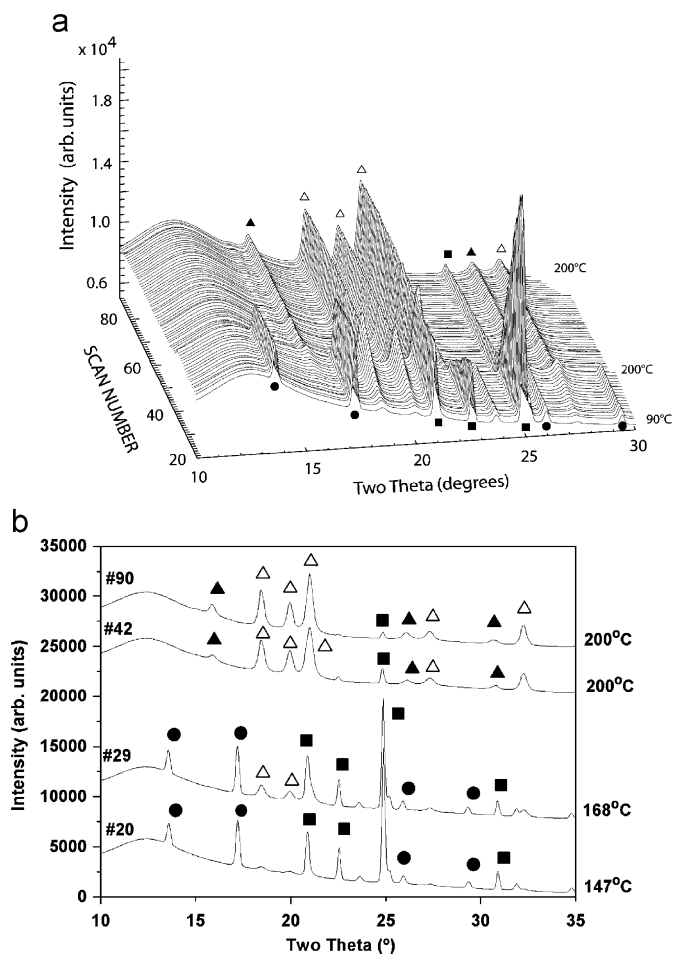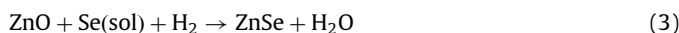$$Zn + H_2O \rightarrow ZnO + H_2 \qquad (1)$$

Fig. 1. (a) Stack of powder diagrams recorded for the "route A" experiment. The stronger peaks of the different phases are marked on the figure. (b) Selected patterns at various temperatures. The following phases were identified: ■ Zn (4-831), ● Se (6-362), △ ZnO (36-1451) and ▲ ZnSe (37-1463). The numbers in the parentheses are the card numbers in the ICCD database.
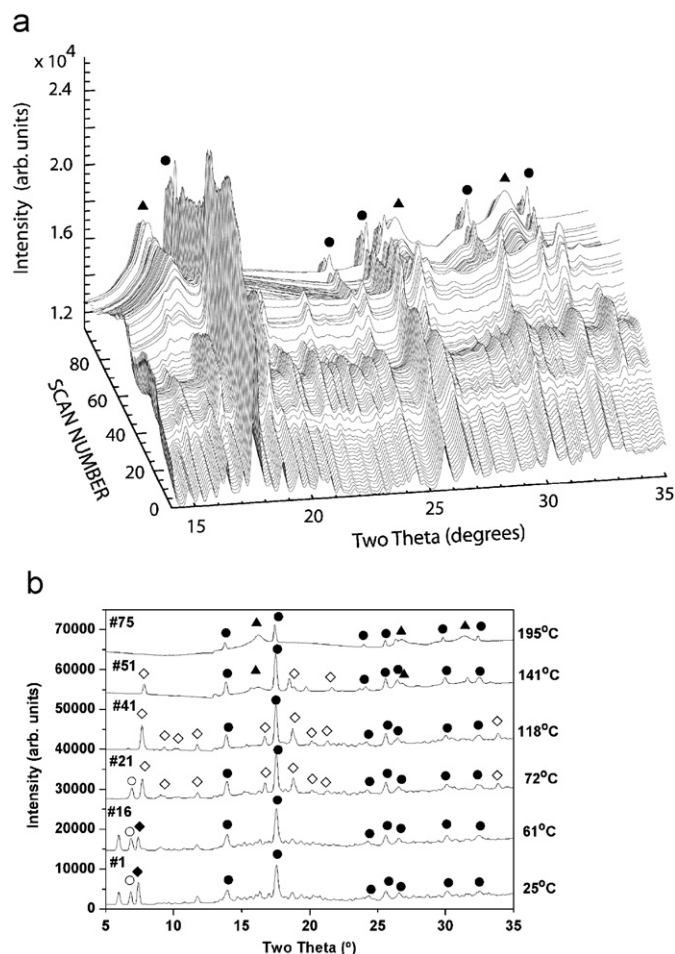

Fig. 2. (a) Stack of powder diagrams recorded for the "route B" experiment. The stronger peaks of the different phases are marked on the figure. (b) Selected patterns at various temperatures. The background scattering has been removed. The following phases were identified: ○ $ZnSO_3 \cdot 2.5H_2O$ (42-97) ◆ $ZnSO_4 \cdot 3Zn(OH)_2$ (44-675), ◇ $NaZn_2OH(SO_3)_2 \cdot H_2O$ (37-20), ● Se (6-362) and ▲ ZnSe (37-1463). The numbers in the parentheses are the card numbers in the ICCD database.

$$Se \rightarrow Se(sol) \tag{2}$$

$$ZnO + Se(sol) + H_2 \rightarrow ZnSe + H_2O \tag{3}$$

$$Zn + Se \rightarrow ZnSe \tag{4}$$

Our data do not give any evidence for the formation of $Zn(OH)_2$ as proposed by Peng et al. [14] and the formation of ZnSe does not go to completion. The sample was found to contain ZnSe, ZnO and Zn after 123 min at 200 °C. The FWHM of the (111) reflection corrected for the instrumental peak broadening revealed an average size of the crystalline domains of 18 nm.

The "route B" experiment is shown in Figs. 2a and b. The sample of composition $ZnCl_2+Se+Na_2SO_3$ in the molar ratio 1:1:1 in water was heated from 25 to 200 °C in 120 min and each pattern was exposed for 40 s. A more complex sequence of reactions is observed in this case. Fig. 2a shows the various phases present during different stages of the synthesis and only the ZnSe and Se phases are marked on this figure, while Fig. 2b shows an identification of the phases present at different selected temperatures. Pattern no. 1 was recorded at 25 °C and it was found to contain $ZnSO_3 \cdot 2.5H_2O$ (42-97), $ZnSO_4 \cdot 3Zn(OH)_2$ (44-675) and Se (6-362) and unidentified phase(s). The same mixture of phases was found at 61 °C (pattern no. 16). $NaZn_2OH(SO_3)_2 \cdot H_2O$ (37-20) forms in the temperature range from 61 and 72 °C and the $ZnSO_4 \cdot 3Zn(OH)_2$ phase and the unidentified phase(s) disappeared

at ca. 72 °C. The $ZnSO_3 \cdot 2.5H_2O$ phase disappears between 72 and 118 °C. The amount of $NaZn_2OH(SO_3)_2 \cdot H_2O$ has decreased considerably at 141 °C and the formation of ZnSe (37-1463) has started at this temperature. The amount of Se decreases between 141 and 195 °C and simultaneously the diffracted intensities from ZnSe increase. Only ZnSe and Se is observed at 195 °C. It is therefore concluded that the reduction of elemental Se by SO_3^{2-} starts between 141 and 195 °C and that the Zn^{2+} ions react directly with the Se^{2-} ions to form ZnSe. The reaction does not go to completion within the time frame of the experiment as it is seen from the relatively large amount of unreacted Se in the last recorded patterns. The average size of crystalline domains of the ZnSe particles is in this case found to be 9 nm. The two in situ experiments show that the ZnSe phase is formed relatively fast under hydrothermal conditions as reaction times of about two hours are sufficient for the formation of this phase. Several crystalline precipitated intermediates were observed in the route B experiment but it should be kept in mind that eventual amorphous intermediates are not directly detected by in situ X-ray powder diffraction as they contribute to the diffuse background scattering.

Several laboratory (ex situ) experiments were carried out with different compositions of the starting mixtures and the results are
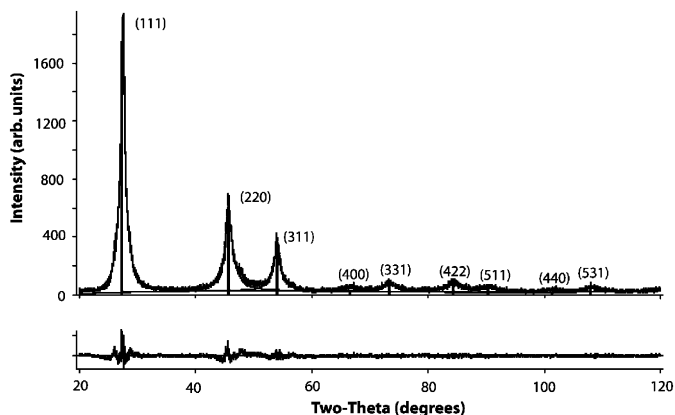
Fig. 3. Observed (crosses) and calculated (solid line) X-ray powder diffraction profiles of nanocrystalline ZnSe prepared from $ZnCl_2$+Se+Na_2SO_3+0.1 M NaOH (experiment **5**) as described in the text. The indexing corresponds to a cubic unit cell with $a = 5.629(3)$Å and the vertical bars represent the refined positions of the Bragg peaks. The lower curve represents the difference the observed and calculated profiles.

Fig. 4. TEM image of nanocrystalline ZnSe prepared from $ZnCl_2$+Se+Na_2SO_3+0.1 M NaOH (experiment **5**) as described in the text.

summarized in Table 1. From Table 1, it is seen that reaction temperatures higher than 170 °C are needed to form the ZnSe phase (experiment **1**) while heating for 24 h at 180 °C results in the formation of ZnSe and unreacted Se when elemental Zn and Se are used as the reactants (experiment **2**). $ZnCl_2$ was used as the Zn source and Na_2SO_3 as the reducing agent in experiments **3–6**. The zinc oxide sulfite hydrate, $Zn_3O_4S \cdot 3H_2O$ (the composition might possibly be $ZnO \cdot ZnSO_3 \cdot 3H_2O$) observed in experiment **3** corresponds to ICCD card no. 3-710. This card does not contain any indexing of the observed reflections and the studied sample might have been multiphased. A definitive identification of the products in this experiment could therefore not be performed. The use of $ZnCl_2$ as the Zn source is advantageous as the formation of ZnO is avoided and ZnSe is formed rapidly. All samples contained unreacted Se in the final product and one sample was therefore heated for 19 h (experiment **6**) but the prolonged reaction time did not minimize the amount of unreacted Se.

The unreacted Se was dissolved by boiling the as prepared sample in a solution made from Na_2SO_3 and 2 M NaOH for about 30 min under reflux. The ZnSe phase was afterwards isolated by centrifugation and decantation, washed with water and thereafter dried. The purified ZnSe sample was then examined by X-ray powder diffraction and TEM. Fig. 3 shows an X-ray powder diffraction pattern of ZnSe prepared from a starting of composition $ZnCl_2$+Se+Na_2SO_3+0.1 M NaOH and heated for 2 h at 185 °C (experiment **5**). The pattern shows that the sample is composed of pure ZnSe phase. The Bragg peaks are substantially broadened and it is therefore concluded that the sample is nanocrystalline. Attempts to analyze the pattern by a conventional Rietveld refinement were unsuccessful because of anisotropic size broadening effects. The three strongest reflections (111), (220) and (311) were used for the determination of the crystalline domain sizes. Using the FWHM values for the (111), (220) and (311) reflections average crystalline domain sizes of 9.3, 6.7 and 7.6 nm were obtained, respectively, giving an average size of the crystalline domains of 7.9 nm. The lattice constant a was determined by performing a least-squares fit to the determined peak positions and a value of $a = 5.629(3)$Å was obtained, which is slightly small than the lattice parameter of bulk crystalline ZnSe ($a = 5.66882(8)$Å) [18] and lower than the lattice constant of $a = 5.66876$Å for nanocrystalline ZnSe obtained by Peng et al. [14]. In the case of metallic nanoparticles, it has been shown that lattice constants often decrease with decreasing particle size
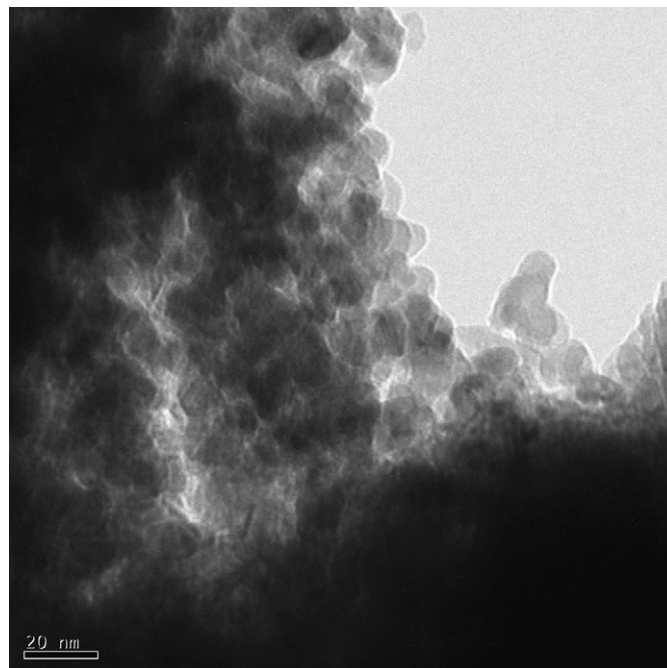
while the reverse effect has been observed in ionic compounds in e.g. CeO_2 [19,20]. The reduced lattice parameter of the prepared ZnSe nanoparticles might alternatively be caused by oxygen impurities.

A total of ten TEM images were recorded of samples taken from the batch used for measuring the sample X-ray powder diffraction pattern shown in Fig. 3 (experiment **5**). Fig. 4 shows a representative TEM image showing relatively large aggregates of nanoparticles, which makes an accurate size determination of the nanoparticle difficult. From Fig. 4, it is seen that the nanoparticles have typical dimensions of approximately 10 nm, which is in fair agreement with the sizes of the crystalline domains obtained by X-ray powder diffraction.

4. Conclusion

Hydrothermal synthesis of nanocrystalline ZnSe has been studied by *in situ* X-ray powder diffraction using synchrotron radiation. This study showed that nanocrystalline ZnSe is formed directly when Zn and Se are used as the reactants and ZnO is in this case formed as a by-product (route A). A complex reaction path was observed when $ZnCl_2$, Se and Na_2SO_3 were used as the starting materials and ZnSe and Se were the only crystalline phases in the obtained product (route B). Nanocrystalline ZnSe was also synthesized *ex situ* using the route A and B methods and characterized by conventional X-ray powder diffraction and TEM. An average crystalline domain size of ca. 8 nm was determined by X-ray powder diffraction and in fair agreement with the TEM images, which showed larger aggregates of nanoparticles of approximate diameters of 10 nm. Finally, we conclude that *in situ* X-ray powder diffraction using synchrotron radiation is able to provide detailed information on chemical reactions occurring in a variety of solid/liquid and solid/gas systems as well as on hydrothermal reactions. The method has successfully been applied for studies of construction materials such as gypsum and concrete and hydrogen storage materials [21,22]. It is also

potentially useful within the field of biomineralization e.g. studies of the hydrothermal formation of $CaCO_3$ [23].

Acknowledgments

References

[1] C.C. Chen, A.B. Herhold, C.S. Johnson, A.P. Alivisatos, Science 276 (1997) 398–401.
[2] L. Motte, F. Billoudet, E. Laxaze, J. Douin, M.P. Pleni, J. Phys. Chem. B 101 (1997) 138–144.
[3] J. Yang, F.C. Meldrum, J.H. Fendler, J. Phys. Chem. 99 (1995) 5500–5504.
[4] N. Herron, Y. Wang, H. Echert, J. Am. Chem. Soc. 112 (1990) 1322–1326.
[5] I.L. Medintz, H.T. Uyeda, E.R. Goldman, H. Mattoussi, Nat. Mater. 4 (2005) 435–446.
[6] R.C. Somers, M.G. Bawendi, D.G. Nocera, Chem. Soc. Rev. 36 (2007) 579–591.
[7] B.P. Zhang, T. Yasada, Y. Segawa, H. Yaguchi, K. Onabe, E. Edamatsu, T. Itoh, Appl. Phys. Lett. 70 (1997) 2413–2415.
[8] M.C.H. Liao, Y.H. Chang, Y.F. Chen, J.W. Hsu, J.M. Lin, W.C. Chou, Appl. Phys. Lett. 70 (1997) 2256–2258.
[9] E.D. Bourret-Courchesne, Appl. Phys. Lett. 68 (1996) 2418–2420.
[10] M. Abdel Rafea, J. Mater. Sci.: Mater. Electron. 18 (4) (2007) 415–420.
[11] Y. Jiao, D. Yu, Z. Wang, K. Tang, X. Sun, Mater. Lett. 61 (2007) 1541–1543.
[12] G.N. Karanikolos, N.-L. Law, R. Mallory, A. Petrou, P. Alexandridis, T.J. Mountziaris, Nanotechnology 17 (13) (2006) 3121–3128.
[13] N. Pradhan, X. Peng, J. Am. Chem. Soc. 129 (2007) 3339–3347.
[14] Q. Peng, Y. Dong, Z. Deng, X. Sun, Y. Li, Inorg. Chem. 40 (2001) 3840–3841.
[15] S. Yochelis, G. Hodes, Chem. Mater. 16 (2004) 2740–2744.
[16] H. Qian, X. Qiu, L. Li, J. Ren, J. Phys. Chem. B 110 (2006) 9034–9040.
[17] A.P. Hammersley, ESRF Internal Report, ESRF97HA02T, "FIT2D: An introduction and Overview," 1997.
[18] H. McMurdie, et al., Powder Diffr. 1 (1986) 345.
[19] W.H. Qi, M.P. Wang, Y.C. Su, J. Mater. Sci. Lett. 21 (2002) 877–878 and references therein.
[20] F. Zhang, S.-W. Chan, J.E. Spanier, E. Apak, Q. Jin, R.D. Robinson, I.P. Herman, Appl. Phys. Lett. 80 (2002) 127–129.
[21] A.N. Christensen, T.R. Jensen, B. Lebech, J.C. Hanson, H.J. Jakobsen, J. Skibsted, Dalton Trans. 4 (2008) 455–462.
[22] L. Mosegaard, B. Møller, J.-E. Jørgensen, Y. Filinchuk, Y. Cerenius, J.C. Hanson, E. Dimasi, F. Besenbacher, T.R. Jensen, J. Phys. Chem. C 112 (2008) 1299–1303.
[23] S.B. Mukkamala, C.E. Anson, A.K. Powll, J. Inorg. Biochem. 100 (2006) 1128–1138.